Biomacromolecules **2007,** *8,* 1131−1137

In Situ Copolyesters Containing Poly(L-lactide) and Poly(hydroxyalkanoate) Units

Dahlia Haynes,[†] Nilmini K. Abayasinghe,[†,||] Graham M. Harrison,[‡] Karen J. Burg,[§] and Dennis W. Smith, Jr.*,[†]

Department of Chemistry, Department of Chemical Engineering, and Department of Bioengineering, Center for Advanced Engineering Fibers and Films, Clemson University, Clemson, South Carolina 29634-0973

Received October 24, 2006; Revised Manuscript Received December 31, 2006

In situ copolyesters containing polylactide (PLA) and polyhydroxyalkanoate (PHA) segments were obtained via ring-opening polymerization of L-lactide using PHA as a macroinitiator with stannous octoate as catalyst. Incorporation of PHA (20 wt %) into PLA affords a novel copolymer with M_n values ranging from 25 to 50 KDa and low polydispersities of 1.8−2.3. DSC analysis of the copolymer indicates well-defined crystallization and melting transitions different from the homopolymers and corresponding blend. The polymers were characterized by FT-IR, GPC, DSC, optical microscopy, NMR, and TGA. The results show successful reactivity of PHA as a macroinitiator for the ring-opening polymerization of lactide.

Introduction

Environmental and sustainability issues concerning petroleum-based feed stocks have begun a growing emphasis on the opportunity of renewable resource and biodegradable materials for plastics and fibers including pharmacological,[1] biomedical,[2,3] agricultural,[4] and food packaging[5] applications. Poly(lactic acid) (PLA) (Scheme 1a), based on corn-derived lactic acid and lactide monomer, has emerged as the leading renewable thermoplastic resin.[6−8] The ability of PLA to successfully compete in broad applications with commodity plastics, however, is limited in part due to its hard/brittle properties, poor elongation, and poorly placed (ca. 50−60 °C) glass transition temperature. Commercial production and expanding applications of PLA continue in many countries with Natureworks LLC as the leading U.S. manufacturer.[8]

A key advantage of lactide is its ability to be enhanced or modified via copolymerization,[9−12] well-defined stereopolymerization,[13,14] and/or blending.[15] Enhancing the properties and performance of polymers formed from lactide can significantly increase its use. Modification through copolymerization with another biodegradable resin can offer an attractive way to improve upon the properties of polymer products containing PLA targeted for specific applications.

Polyhydroxyalkanoates (PHA) have also been extensively studied for a variety of commercial applications (Scheme 1b) and include a broad class of biocompatible thermoplastic polyesters produced by bacteria under careful growth and nutrient restrictions.[16] Based on the ability of PHA to degrade in aerobic and anaerobic conditions, PHA has renewed interest, focused primarily in biomedical and commodity plastic applications.[16−20] Broader applications of PHAs, however, are limited due to thermal degradation at high processing temperatures (presumably via random-scission reactions occurring through a β-mechanistic pathway), its blend compatibility, and production costs of the fermentation processes.[17]

Scheme 1. Structures of PLA (a) and PHA (b)

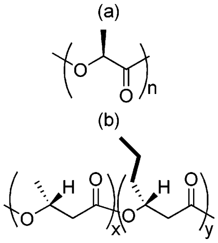

Alternative strategies are of renewed interest to improve the applicability of this class of materials. Linear polylactide (PLA) exhibits a T_g of ca. 60 °C and a melting transition of approximately 170 °C, whereas the T_g of PHA is approximately between −10 and 0 °C, and its melting points range between 160 and 180 °C. Proctor and Gamble Co. has recently investigated the properties of alloys consisting of PLA and PHA for improving the drawbacks of each while maintaining their intrinsic advantages.[18] Efforts toward enhancing the thermomechanical and processing properties of both classes of polymers have focused on blending PHA and PLA to produce the most promising biodegradable materials for use in a variety of applications.

Previous studies have used $Sn(Oct)_2$ as an effective and widely used catalyst for the ring-opening polymerization of L-lactide.[19] The use of tin catalysts have been shown to produce high molecular weight polylactide with low polydispersities and a minimum of side reactions. Here, we report the in situ polymerization of lactide initiated by PHA/$Sn(Oct)_2$ to produce the first copolymer of PLA and PHA (**1**). PHA/PLA copolymers wherein a covalent link is made between the two different polyester chains were not known previously.

---

* To whom correspondence should be addressed. E-mail: dwsmith@clemson.edu.

[†] Department of Chemistry.

[‡] Department of Chemical Engineering.

[§] Department of Bioengineering.

[||] Current address: Mermet Technologies, Inc., Spartenburg, SC.

10.1021/bm061018q CCC: $37.00

Table 1

copolymer	PHA feed wt % (NMR)[a]	M_n[b] ($\times 10^{-3}$)	M_w/M_n[b]	T_m[g] (°C)	ΔH_m[g] (J/g)	T_c[g] (°C)	ΔH_c[g] (J/g)	T_g (°C)	% cryst.[e]	T_d[f]
PLLA	n/a	35	2.0	176	41	111	34	61	49	272
PHA	100 (100)	126	2.4	126, 145	3, 31	62	26	−1	n/a	283
blend	20 (20)	46	3.7	143,[c] 173[d]	6,[c] 40[d]	46,[c] 94[d]	4,[c] 5[d]	−2[c]	48	286
1	20 (19)	29	2.3	170	34	84	11	56	40	269

[a] Calculated from ^{1}H NMR. [b] Determined by GPC. [c] Peak associated with PHA. [d] Peak associated with PLA. [e] Calculated from 100% crystalline PLA and DSC. [f] Determined by TGA. [g] Determined by DSC.

Scheme 2. Synthesis of PHA-*co*-PLA Copolymer **1** from PHA and L-Lactide

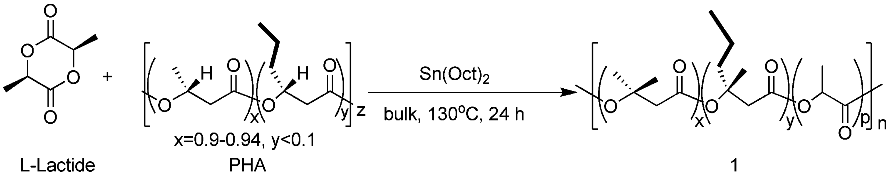

Experimental Section

General. ^{1}H NMR 300 MHz and proton decoupled ^{13}C NMR 125 MHz spectra were obtained using the Bruker AF-300 spectrometer system. Chloroform-*d* was used as solvent, and chemical shifts reported were internally referenced to tetramethylsilane (0 ppm) and $CDCl_3$ (77 ppm) for ^{1}H and ^{13}C nuclei, respectively. Gel permeation chromatography (GPC) data were collected in $CHCl_3$ using a Waters Alliance refractive index detector at 35 °C and equipped with Polymer Labs PLGel 5 mm Mixed-C and Mixed E columns. Retention times were calibrated against Polymer Labs Easical PS-2 polystyrene standards.

Thermal gravimetrical analysis (TGA) data were obtained from a Mettler-Toledo 851 TGA/SDTA system at a heating rate of 10 °C/min in a nitrogen atmosphere. Differential scanning calorimetry (DSC) was obtained from TA instruments Q1000 system with an auto sampler and liquid nitrogen cooling system. Analysis was carried out using TA Instruments Universal Analysis Software. The glass transition (T_g) was obtained from a second heating curve after cooling at 10 °C/min. The reported T_g value was taken at the midpoint of the C_p curve.

Viscoelastic measurements were performed using a Rheometric Scientific ARES. Samples were tested using a cone and plate geometry with a diameter of 25 mm where dynamic strain and frequency tests were conducted at a temperature of 165 °C.

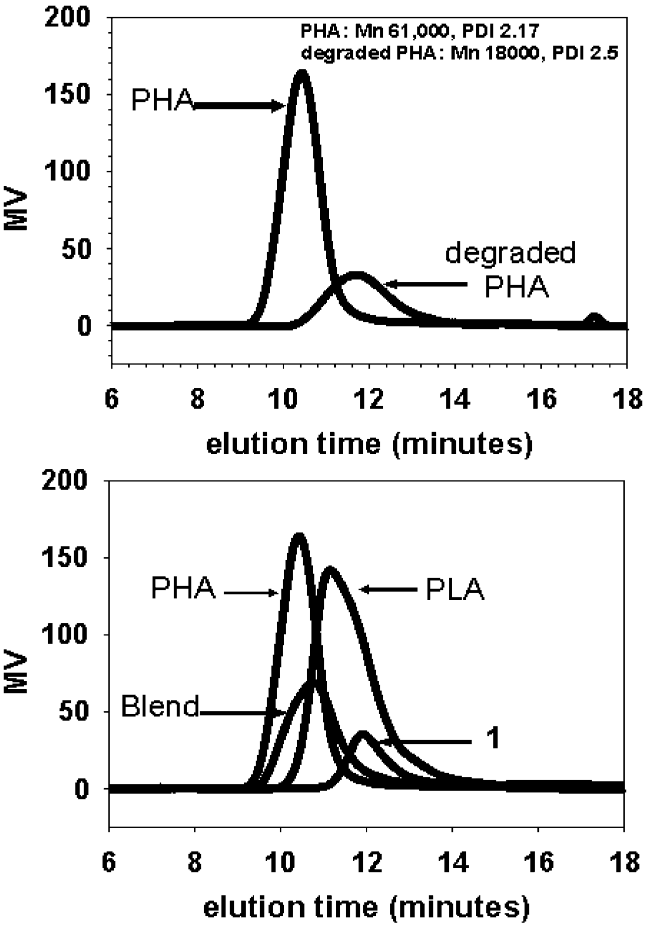

Figure 1. (a) GPC curves for PHA and degraded PHA; and (b) GPC curves for PHA, PLA, PHA-*co*-PLA (**1**), and PHA/PLA blend.

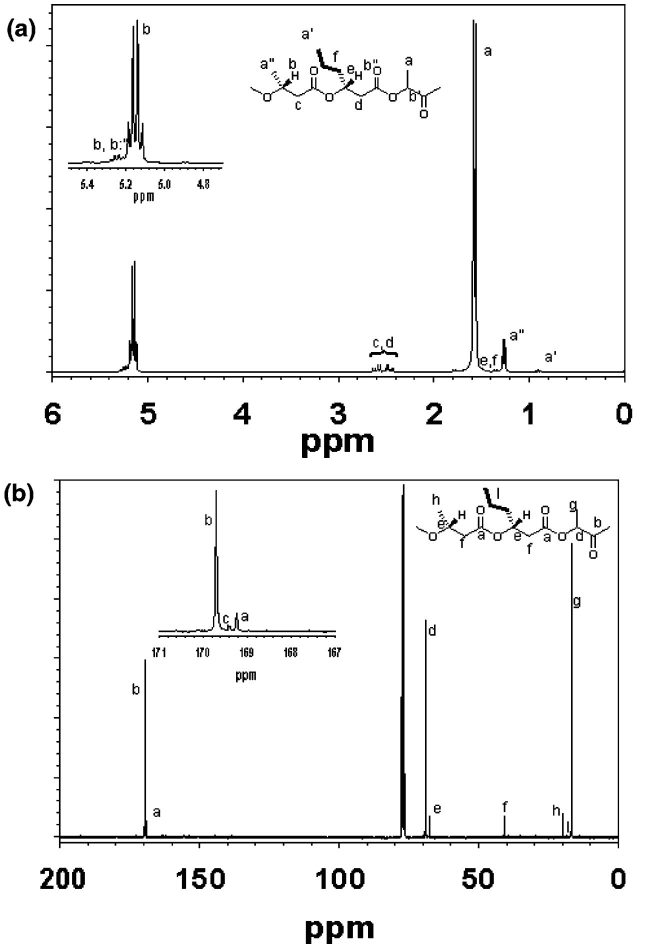

Figure 2. ^{1}H NMR spectrum of melt prepared PHA-*co*-PLA copolymer **1** (a) and ^{13}C NMR spectrum of solution prepared **1** (b).

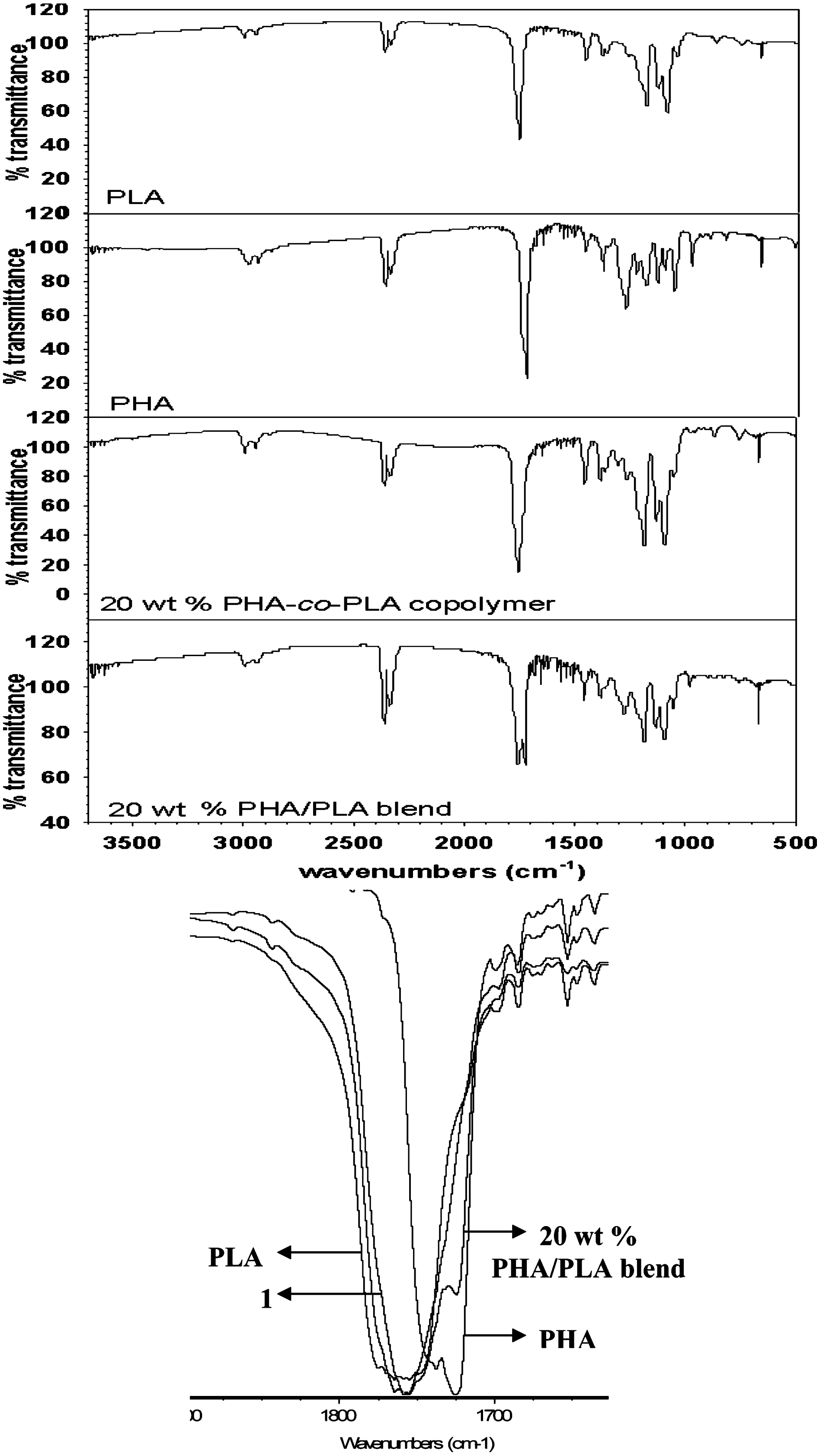

Figure 3. FTIR spectra of PLA, PHA, PHA-*co*-PLA copolymer **1**, and 20 wt % PHA/PLA blends.

Spherulite morphologies and crystal growth were characterized on a Nikon SMZ-U microscope utilizing linear polarized light, with an attached Mettler FP82HT hotstage at which samples were brought to 170 °C, remained at isothermal point for 5 min, and then allowed to cool at a rate of 5 °C/min. Digital images were captured and analyzed using Image Pro Plus (4.0) software at 10k magnification.

Fourier transform infrared (FTIR) spectroscopy was performed on thin films using a ThermoNicolet Magna-IR 550 FTIR spectrometer

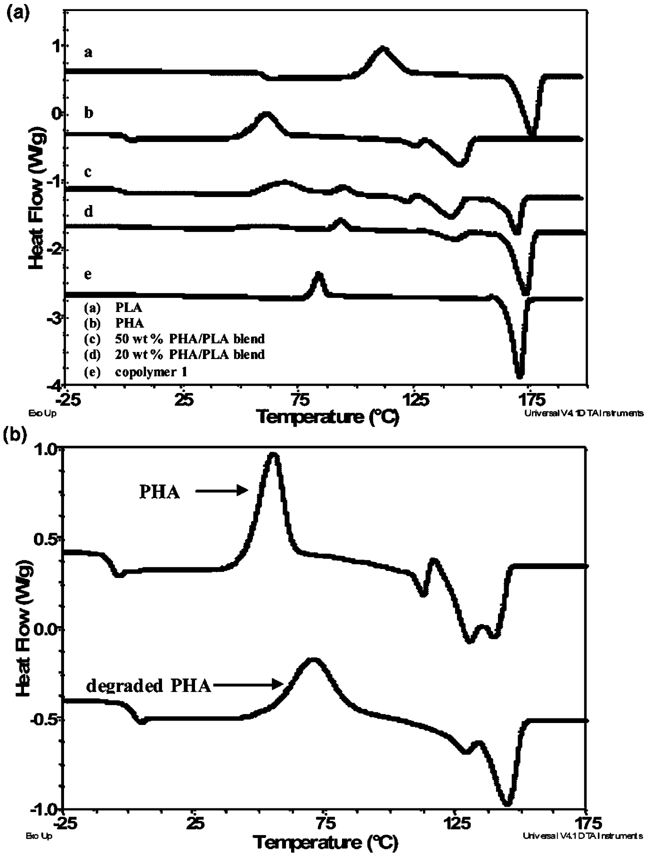

Figure 4. (a) DSC curves (second heating) for melt prepared PHA-*co*-PLA copolymer **1**, the 20 wt % PHA/PLA blend, PHA, and PLA. (b) DSC curves (second heating) of PHA and degraded PHA.

equipped with a Nic-Plan microscope, with a resolution of 2 cm^{-1} using 16 scans.

Surface topologies were obtained using a scanning electron microscope (Hitachi S-800) upon which samples were coated with platinum before being mounted.

Materials. Poly(3-hydroxybutyrate-*co*)-3-hydroxyhexanoate samples were generously supplied by Proctor and Gamble Co. under the tradename, NODAX. Lactide, stannous octoate ($Sn(Oct)_2$), chloroform-*d*, and toluene were purchased from Aldrich or Fisher Scientific. All reaction manipulations were conducted under nitrogen or argon. Solvents were dried using standard procedures.[20]

Melt Copolymerization of PHA with L-Lactide (1). To a 5 mL glass ampule were added poly(3-hydroxybutyrate-*co*)-3-hydroxyhexanoate (M_n = 126 000, 0.2 g), L-lactide (0.8 g), and $Sn(Oct)_2$ (100 μL of 0.01 mol L^{-1} solution in anhydrous toluene) under nitrogen. The ampule was heated to facilitate mixing and sealed under vacuum. The tube was then immersed in an oil bath at 130 °C for 24 h. The crude product was dissolved in chloroform, precipitated into both methanol and hexane repeatedly, and then dried in vacuo to afford a white fibrous material. Yield: >90%. FTIR (neat film) (cm^{-1}): 756, 870, 978, 1050, 1092, 1131, 1185, 1268, 1304, 1362, 1383, 1453, 1684, 1758, 2894, 2944, 2994. ^{1}H NMR (300 MHz, $CDCl_3$) δ (ppm): 5.2 (q, J = 6.88 Hz, 1H, β-H, PHA), 5.1 (q, J = 7.24 Hz, 3.16H, α-H, LA), 2.5 (dq, J = 15.48, 7.24 Hz, 1.59H, α-H, PHA), 1.56 (d, J = 6.88 Hz, 15.06, CH_3, LA), 1.25 (d, J = 6.19, 1.26H, CH_3, PHA), 0.88 (t, J = 7.24 Hz, 0.16H, $-CH_2CH_3$, PHA). ^{13}C NMR (500 MHz, $CDCl_3$) δ (ppm): 169.71, 169.43, 169.25, 69.10, 67.70, 40.86, 19.86, 18.42, 16.73. See Table 1 for other characterization details.

Solution Copolymerization of PHA with L-Lactide (20% PHA-*co*-PLA Copolymer). To a 5 mL ampule were added toluene (0.5 mL), poly(3-hydroxybutyrate-*co*)-3-hydroxyhexanoate (M_n = 126 000, 0.2 g), L-LA (0.8 g), and $Sn(Oct)_2$ (100 μL of 0.01 mol L^{-1} solution in anhydrous toluene) under nitrogen. The ampule was then heated slowly to facilitate mixing. The ampules remained under nitrogen while being immersed in an oil bath at 80 °C for 24 h. The crude product was dissolved in chloroform and precipitated into both swirling hexane and methanol repeatedly. The resulting polymer was dried in vacuo to afford a white fibrous material. Yield: >90%. FTIR (neat film) (cm^{-1}): 756, 870, 978, 1050, 1092, 1131, 1185, 1268, 1304, 1362, 1383, 1453, 1684, 1758, 2894, 2944, 2994. ^{1}H NMR (300 MHz, $CDCl_3$) δ (ppm): 5.2 (q, J = 6.88 Hz, 1H, β-H, PHA), 5.1 (q, J = 7.24 Hz, 4.12H, α-H, LA), 2.5 (dq, J = 15.48, 7.24 Hz, 1.11, α-H, PHA), 1.56 (d, J = 6.88 Hz, 14.12, CH_3, LA), 1.25 (d, J = 6.19, 2.99H, CH_3, PHA), 0.88 (t, J = 7.24 Hz, 0.14H, $-CH_2CH_3$, PHA). ^{13}C NMR (500 MHz, $CDCl_3$) δ (ppm): 169.71, 169.43, 169.25, 69.10, 67.70, 40.86, 19.86, 18.42, 16.73. See Table 1 for other characterization details.

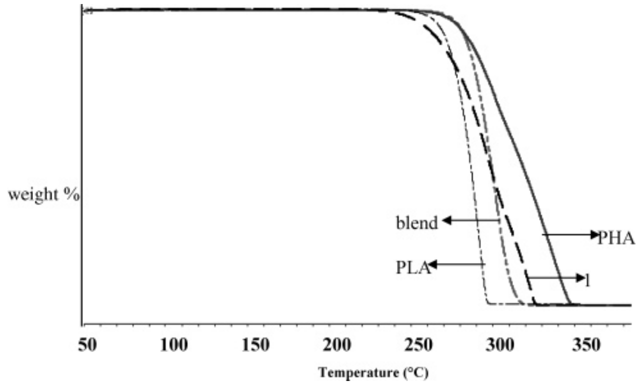

Figure 5. Thermal degradation curves for PHA-*co*-PLA copolymer **1**, PLA, PHA, and the corresponding 20 wt % PHA/PLA blend.

Blends of PLLA and PHA (20% PHA/PLLA). Solution blending was obtained by using the designated weight percentages of PHA and PLLA dissolved in a minimal amount of $CHCl_3$ (10 wt % solutions). The mixtures were then precipitated in cold, swirling methanol, then hexane, and the resulting polymer blend was dried in vacuo. Analysis was then performed and compared to the copolymer prepared in situ.

Results and Discussion

Novel PLA/PHA copolymers (**1**) were prepared by the ring-opening polymerization of lactide in the presence of commercial PHA as shown in Scheme 2. Variable ratios of PHA and lactide were investigated, and copolymers of PLA with 20 wt % PHA were chosen for further studies on the basis of initial properties and comparison with blend studies.[8] Copolymers were synthesized in the presence of $Sn(Oct)_2$ (0.01 wt %) and reacted for 24 h at 130 °C with or without anhydrous toluene. Both solution and melt methods gave white fibrous polymer in high yield upon precipitation and show similar properties, with slightly higher molecular weights obtained for the melt process (Table 1).

The corresponding values obtained from GPC for PHA, PLA, 20 wt % PHA/PLA blend, and in situ PHA-*co*-PLA copolymer **1** are summarized in Table 1. In situ copolymerization resulted in an overall decrease of PHA molecular weight from M_n = 126 000 to 29 000 for the new copolyester as determined by GPC. The molecular weight dropped significantly possibly due to random chain scission reactions known to occur at high temperatures for PHA copolymers.[8] To investigate the effects of catalyst and heat on the high molecular weight PHA starting polymer, control degradation of PHA alone in the presence of $Sn(Oct)_2$ (0.01 wt %) at 130 °C for 24 h was performed to help account for the decrease in molecular weight of copolymer **1**. Figure 1a shows GPC chromatograms of starting and degraded PHA where the decrease in molecular weight is significant (M_n from 61k to 18k) and suggests that interchange or transesteri-

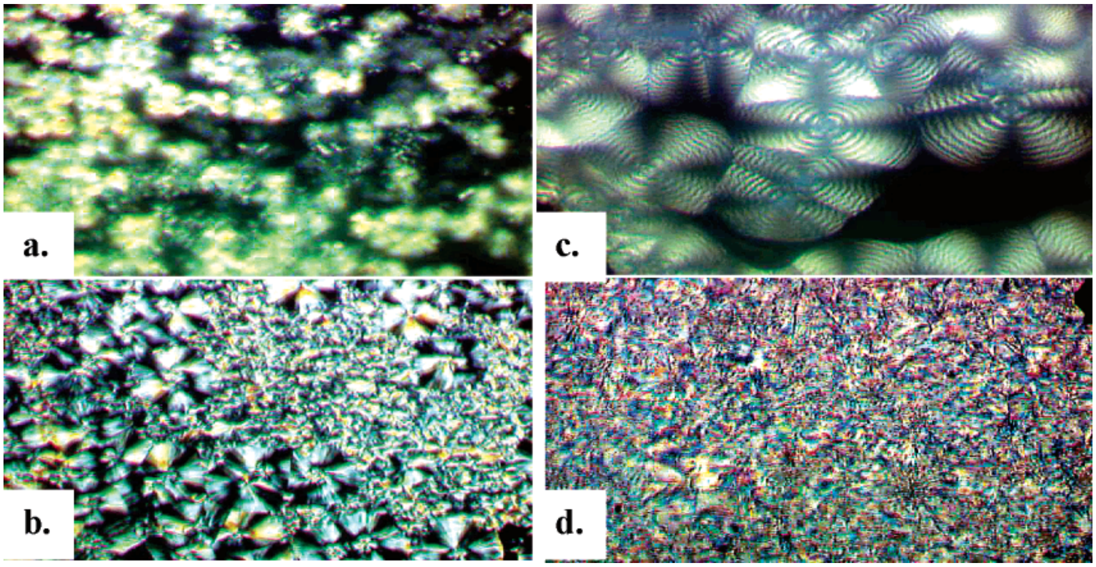

Figure 6. Polarized optical micrographs at 10k magnification showing spherulitic morphology of PLA (a), 20 wt % PHA/PLA blend (b), PHA (c), and 20 wt % PHA/PLA copolymer **1** (d) crystallized at 165 °C.

fication reactions can occur during in situ polymerization. The control degraded PHA was also analyzed by DSC and illustrates that the thermal behavior of the degraded PHA is much different from that of copolymer **1** (Figure 4b). Transesterification is known to occur in molten polyesters in addition to other chain scission and recombination reactions and is used to prepare a homogeneous random copolymer between two immiscible polyesters.[21−26] The mechanism of transesterification remains somewhat ambiguous in many reported studies; however, several approaches have been published on the kinetics of a transesterification reaction through detailed NMR and IR spectroscopy analyses.[27−31]

After copolymerization with lactide, copolymer **1** exhibits a polydispersity ($M_w/M_n = 2.3$) typically found between that for PLA and PHA homopolymers. The corresponding blend shows a higher polydispersity of 3.7 as compared to copolymer **1** (Table 1). Elution time curves from GPC are compared and shown in Figure 1b. The GPC results indicate significant chain cleavage of PHA, suggesting that lactide segments could then grow from multiple initiation sites in addition to transesterification reactions.

The ^{1}H and ^{13}C NMR spectra for the 20 wt % PHA/PLA copolymer (**1**) are shown in Figure 2a and b. Signals at δ 5.1 and 1.56 ppm in the ^{1}H NMR spectrum represent the methyl and methylene protons of the lactide linkage, respectively, while signals at δ 5.2 and 1.25 ppm represent the methyl and β-protons of the PHA units. The compositions were determined by the integration ratio of the PLA methyl protons at δ 1.56 with those of the methyl protons from PHA at δ 1.25. The actual ratio calculated by NMR is consistent with the feed ratio as shown in Table 1. The ^{13}C NMR spectrum was analyzed using the expanded signals from the carbonyl region. New ester carbonyl signals that differ from both parent polymers are found.

Films of PLLA, PHA, PHA-*co*-PLA copolymer **1**, and its corresponding 20 wt % PHA/PLA blend were evaluated by FTIR analysis, and the results are shown in Figure 3. The characteristic peaks of the C=O bands for PHA, PLA, the blend, and **1** are observed from 1600 to 1700 cm^{-1}, where PHA has peaks at 1738 and 1725, and PLA at 1755 cm^{-1}. The C=O band occurring at 1758 cm^{-1} for the copolymer is much sharper than that of the C=O stretching bands of PHA and PLA alone. The blend of PLA and PHA clearly shows the overlapping of both respective C=O broad bands, whereas copolymer **1** exhibits a sharper single band. The copolymer **1** fingerprint region, observed at 800−1500 cm^{-1}, also shows formation of new peaks that are suggestive of new C−H (1375−1450 cm^{-1}) and C−O (1300−1100 cm^{-1}) vibrations, which appear in copolymer **1** and which are clearly distinctive from that of PLA and PHA and the blend.

The DSC data for PLA, PHA, copolymer **1**, the corresponding 20 wt % blend, and a 50 wt % blend are shown in Figure 4a. The step transition at 61 °C is attributed to the glass transition temperature of PLA with a crystallization peak at 111 °C and a melting peak at 176 °C. PHA exhibits a glass transition temperature at −1 °C, a crystallization peak at 62 °C, and two melting peaks at 126 and 145 °C. The 50 wt % blend shows clearly the separate glass, crystallization, and melting transitions representative of the PHA and PLA polymers. In comparison to copolymer **1**, the 20 wt % blend of PHA/PLA shows expected results where the T_g of PHA alone is visible at −2 °C; the crystallization peak of the blends shows a broad transition at 46 °C that overlaps with the T_g for PLA and another T_c corresponding to the PLA transition at 94 °C. The distinct melting peaks are also visible at 143 and 173 °C for PHA and PLA, respectively. For copolymer **1**, the second heating scan shows one sharp crystallization peak at 84 °C, melting peak at 170 °C, and a very broad glass transition temperature with center around 56 °C. The degree of crystallinity was calculated using the equation:

$$\text{crystallinity (\%)} = (\Delta H_f / \Delta H_f^\circ) \times 100$$

where ΔH_f is the melting enthalpy and $\Delta H_f^\circ = 93$ J/g is the heat of fusion for 100% crystalline PLA.[32] We chose to use the 100% crystalline PLA value as the reference enthalpy for comparison because it is the primary component of the copolymer and blend. The ΔH_f values are obtained from the melting curves of the second heating scans of the DSC. The degree of crystallinity has been reduced by almost 10% from the homopolymer of PLA and its corresponding blend. Thermal properties of the copolymers are summarized in Table 1.

Figure 4b shows the DSC results for the control degradation of PHA and catalyst (SnOct$_2$ @ 130 °C) without lactide. Polymorphic melting generally decreased and became more

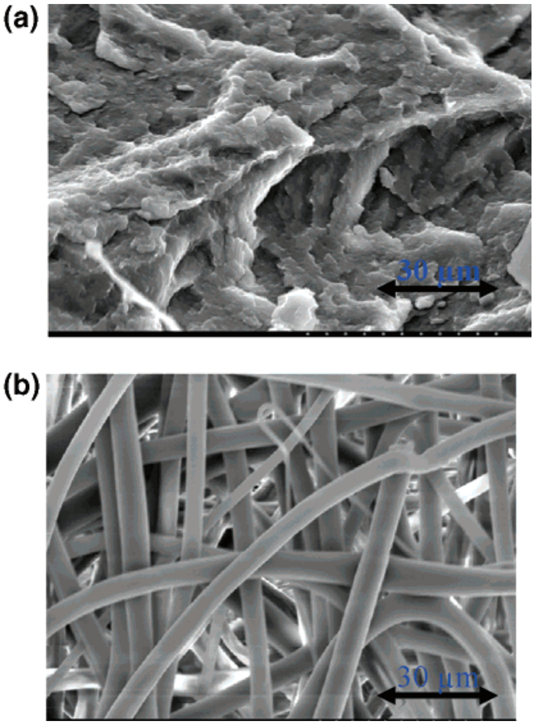

Figure 7. Scanning electron micrograph of cross-section surfaces at 1.0k, 30 μm for melt copolymer **1** solution cast film and electrospun fibers.

disperse with clear melting transitions of 145 and 126 °C for starting PHA to 140, 130, and 113 °C for degraded PHA. The T_g and crystallization temperatures also decreased by at least 5 °C after degradation. The new PHA-*co*-PLA copolymer **1** shown in Figure 4a is not simply degraded PHA or a blend of PLA and PHA, but a new copolymer with clear distinct thermal behavior.

Copolymer **1** exhibited expected thermal stability as shown in Figure 5 by thermal gravimetric analysis (TGA). The copolymer gave a T_d value of 269 °C and is similar to PLA, while PHA has a T_d of 283 °C. The higher molecular weight blend experiences a T_d of 286 °C, giving a higher thermal stability than that of the copolymer **1**.

The optical polarized microscopy of PLLA, PHA, a 20 wt % PHA/PLA blend, and PHA-*co*-PLA copolymer (**1**) is shown in Figure 6. The spherulitic crystal morphology of the novel copolymer differs significantly from that of PHA and PLLA alone. The spherulites of both PHA and PLLA are evident in the blend, suggesting phase immiscibility between the two crystalline domains. The surface topography of the PHA-*co*-PLA copolymer film and fiber was observed by SEM using a cryofractured cross section of the film material and electrospun fiber. Cross-section surfaces in Figure 7a exhibit homogeneous morphology throughout the entire region and fiber width averaged around 7−8 μm as shown in Figure 7b.

Dynamic mechanical characterization was performed on PHA, PLA, and the in situ copolymer **1** to determine its applicability in applications that require rigorous processing conditions. Samples were first subjected to a strain sweep test in which they were deformed at different strain rates and the moduli recorded to determine the linear viscoelastic region (not shown). The samples were then subjected to a frequency sweep at 165 °C. Figures 8 and 9 exhibit the storage and loss moduli and complex viscosity of PLLA, in situ PHA-*co*-PLA copolymer **1** and 20 wt % PHA/PLA blend. The loss modulus is typically higher than the storage modulus for polymers and indicates that the viscous response is stronger than the elastic response where energy stored during deformation is greater than the loss of energy due to changes in the frequency. An increase in the frequency for copolymer **1** shows less change in the storage and loss moduli, whereas the storage and loss moduli of both PLA and PHA (not shown) vary greatly over the range of frequencies. The complex viscosity of PLA and the copolymer is also shown, and the viscosity is reduced in the copolymer as compared to that in the PLA homopolymer.

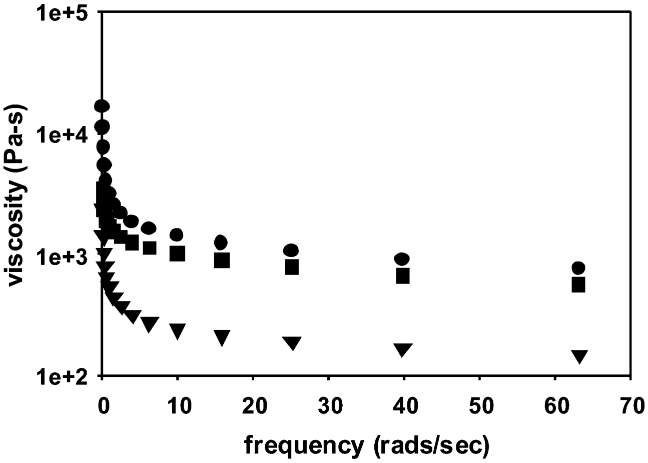

Figure 8. Complex viscosity at 165 °C versus frequency for (●) PLLA, (■) 20 wt % PHA/PLA blend and (▼) PHA-*co*-PLA copolymer **1**.

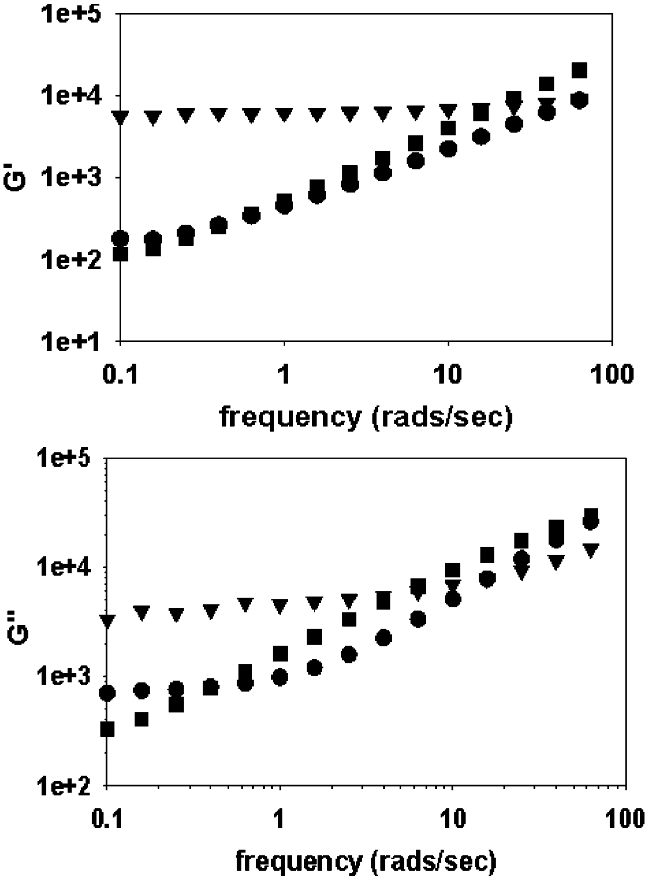

Figure 9. Storage and (b) Loss moduli at 165 °C versus frequency for (●) PLLA, (▼) PHA-*co*-PLA copolymer **1** and (■) 20 wt % PHA/PLA blend.

Conclusions

Lactide was successfully copolymerized with poly(3-hydroxybutyrate-*co*-3-hydroxyhexanoate) (PHA) using a catalytic amount of tin octoate to generate a novel in situ copolyester consisting of both repeating units. Polylactide containing 20 wt % of PHA exhibits significant changes in thermal behavior as shown by DSC. Both the glass transition and the crystallization transition have been altered significantly, indicating formation of a new PLA-*co*-PHA copolymer different from that of its starting materials and respective blend. The polymerization proceeds by random transesterification and competing initiation of lactide, occurring through chain scission reactions of PHA in the presence of $Sn(Oct)_2$ giving a random multiblock copolymer (Scheme 2) with molecular weights ranging from 25k to 50k. The in situ copolymer **1** also imparts improved mechanical properties based on its lower viscosity and dynamic moduli for superior processing conditions as compared to PLA alone that may be useful in a variety of commodity and biomedical applications.

Acknowledgment. We thank the U.S. Department of Education for a GAANN Fellowship to D. Haynes, the National Science Foundation through the Center for Advanced Engineering Fibers and Films (NSF-ERC), and The Department of Commerce through the National Textile Center (NTC). We thank Proctor and Gamble Co. for the generous donation of PHA and Dr. David Melik for helpful advice. D.W.S. is a Cottrell Scholar of Research Corporation.

References and Notes

(1) Winzenburg, G.; Schmidt, C.; Fuchs, S.; Kissel, T. *Adv. Drug Delivery Rev.* **2004**, *56*, 1453−1466.

(2) Ouchi, T.; Shiratani, M.; Jinno, M.; Hirao, M.; Ohya, Y. *Makromol. Chem. Rapid Commun.* **1993**, *14*, 825.

(3) Hayashi, T.; Iwatsuki, M. *Biopolymers* **1990**, *29*, 549.

(4) Ho, K. G.; Pometto, A. L.; Hinz, P. N.; Gadea-Rivas, A.; Bricero, J. A. *J. Environ. Polym. Degrad.* **1999**, *7*, 167−172.

(5) Lagaron J. M.; Cabedo, L.; Cava, D.; Feijoo, J. L.; Gavara, R.; Gimenez, E. *Food Addit. Contam.* **2005**, *22*, 994−998.

(6) Vink, E. T. H.; Rabago, K. R.; Glassner, D. A.; Springs, B.; O'Connor, R. P.; Kolstad, J.; Gruber, P. *Macromol. Biosci.* **2004**, *4*, 551−564.

(7) Vert, M.; Doi, Y.; Stenbuchel, A. *Biopolymers. Polyesters III Applications and Commercial Products*; Wiley−VCH Verlay GrubH: Weinheim, 2002; Vol. 4, p 179.

(8) Noda, I.; Satowski, M. M.; Dowry, A.; Marcott, C. *Macromol. Biosci.* **2004**, *4*, 269−275.

(9) Abayasinghe, N. K.; Glaser, S. K.; Perera, P. U.; Smith, D. W., Jr. *J. Polym. Sci., Part A: Polym. Chem.* **2005**, *43*, 5257−5266.

(10) Edlund, U.; Kaellrot, M.; Albertsson, A.-C. *J. Am. Chem. Soc.* **2005**, *127*, 8865−8871.

(11) Abayasinghe, N. K.; Smith, D. W., Jr. *Macromolecules* **2003**, *36*, 9681−9683.

(12) Saulnier, B.; Ponsat, S.; Coudau, J.; Carreau, H.; Vert, M. *Macromol. Biosci.* **2004**, *4*, 232−237.

(13) Coates, G. W.; Ovitt, T. M. *J. Am. Chem. Soc.* **2002**, *124*, 1316−1326.

(14) Jensen, T. R.; Schaller, C. P.; Hillmyer, M. A.; Tolman, W. B. *J. Organomet. Chem.* **2005**, *690*, 5881−5891.

(15) Huang, M.; Li, S.; Coudane, J.; Vert, M. *Macromol. Chem. Phys.* **2003**, *204*, 1994−2001.

(16) Lenz, R. W.; Gross, R. A.; Fuller, R. C.; Brandl, H. *Prog. Biomed. Eng.* **1988**, *5*, 19−26.

(17) Noda, I.; Green, P.; Satowski, M. K.; Schectman, L. A. *Biomacromolecules* **2005**, *6*, 580−586.

(18) Noda, I.; Satowski, M.; Dowry, A. E.; Marcott, C. *Macromol. Biosci.* **2004**, *4*, 269−275.

(19) Kowalski, A.; Duda, A.; Penczek, S. *Macromolecules* **2000**, *33*, 7359−7370.

(20) Schrek, K. M.; Hillmyer, M. A. Block copolymers and melt blends of polylactide with Nodax microbial polyesters: preparation and mechanical properties. Submitted for publication, personal communication.

(21) Kenwright, A. M.; Peace, S. K.; Richards, R. W.; Bunn, A.; MacDonald, W. A. *Polymer* **1999**, *40*, 5851.

(22) Flory, P. J. *J. Am. Chem. Soc.* **1981**, *103*, 918.

(23) Slivniak, R.; Domb, A. J. *Macromolecules* **2005**, *38*, 5545.

(24) Suzuki, Y.; Han, C. D. *Macromolecules* **2006**, *39*, 3865.

(25) Radmarn, B.; Dadmun, M. D. *J. Polym. Sci.* **2001**, *80*, 2583

(26) Ho, J. C.; Wei, K. H. *Polymer* **1999**, *40*, 717.

(27) Jayakannan, M.; Anilkimar, P. *J. Polym. Sci., Part A: Polym. Chem.* **2004**, *42*, 3996.

(28) McCabe, R. W.; Taylor, A. *Tetrahedron* **2004**, *60*, 765.

(29) Csihony, S.; Beaudette, T. T.; Sentman, A. C.; Nyce, G. W.; Waymouth, R. M.; Hedrick, J. L. *Adv. Synth. Catal.* **2004**, *346*, 1081.

(30) Devaux, J.; Godard, P.; Mercier, J. P. *J. Polym. Sci., Part B: Polym. Phys.* **1982**, 1901.

(31) Messman, J. M.; Storey, R. F. *J. Polym. Sci., Part A. Polym. Chem.* **2004**, *42*, 6238.

(32) Ouchi, T.; Miyazaki, H.; Arimura, H.; Tasaka, F.; Hamada, A.; Ohya, Y. *J. Polym. Sci., Part A: Polym. Chem.* **2002**, *40*, 1218.

BM061018Q